Dynamics of atoms in a femtosecond optical dipole trap

Denis N. Yanyshev,[1,*] Victor I. Balykin,[2] Yulia V. Vladimirova,[1] and Victor N. Zadkov[1]
[1]*International Laser Center and Faculty of Physics, Lomonosov Moscow State University, Moscow 119991, Russia*
[2]*Institute of Spectroscopy, Russian Academy of Sciences, Fizicheskaya 5, Troitsk, Moscow region 142190, Russia*
(Received 14 December 2012; published 11 March 2013)

The semiclassical theory of atomic dynamics in a three-dimensional pulsed optical dipole trap formed by superimposed trains of short laser pulses (down to a few fs duration), which is based on a stochastic formulation for the dynamics of an open quantum system, is considered in detail. It covers all key features of the atomic dynamics in the trap, including the dipole-dipole interaction (DDI) between trapped atoms due to the exchange of virtual photons between the atoms. Analytical solutions are obtained for the relaxation and laser Liouvillians, which describe the dissipation and laser excitation in the system, respectively. The probabilities of single-atom and two-atom escapes from the trap are analyzed. As an example, the theory is applied to computer simulation of Rb atoms preliminarily cooled in a magneto-optical trap that are trapped in a femtosecond optical dipole trap (pulse duration 100 fs). Our simulations prove that such a trap effectively confines atoms at the pump laser power in the range from a few mW to several kW. It is also shown that a near-resonant DDI, through which atoms that are closely spaced in the micropotential wells interact with each other, can be significantly increased by illuminating the atoms with a near-resonant probe laser beam. By varying both the parameters of the trap and the intensity of the probe laser field, the role of the DDI in the atomic dynamics in the trap and its influence on the single-atom and two-atom escape rates are clarified in detail.

DOI: 10.1103/PhysRevA.87.033411 PACS number(s): 37.10.De, 37.10.Gh, 37.10.Vz

I. INTRODUCTION

For more than three decades since the pioneering proposal by Letokhov to trap cold atoms in one dimension by using a standing light wave [1], the manipulation of laser-cooled neutral particles (atoms and, recently, molecules) based on the dipole force exerted by light has become a widely used and powerful tool in experiments studying such single particles and the physics of their interaction with each other and with light [2–5]. Optical dipole traps that are created by superimposing two counterpropagating laser beams or one laser beam superimposed with its mirror reflection form a one-dimensional potential lattice (the so-called optical lattice), and they can easily be made, for instance, two-dimensional by using two pairs of counterpropagating laser beams whose propagation directions are either perpendicular or form a nonzero angle. Nowadays, such optical lattices are being used as a very promising tool for experiments with ultracold atoms, for studying the physics of quantum information processing, for strongly interacting many-body systems on a lattice, etc. [6].

As of now, most optical dipole traps realized experimentally use a continuous-wave (cw) laser that is very far detuned from the atomic resonance of the trapped atoms (the so-called "far-off-resonance trap" or FORT). Despite its obvious advantage as a very simple and reliable device, a cw FORT also has an essential drawback—atoms in such a trap always interact with the field of the laser beam that forms the trap and perturbs atomic states via ac Stark interaction. This leads to the problem of systematic frequency shift, which can be solved for some atomic transitions by using the so called "magic wavelength" configuration [7,8]. However, the existence of such a wavelength is accidental and the strategy of the "magic wavelength" is thus not a universal one.

One can remove these disadvantages by replacing a cw pump laser beam forming the trap with a train of short (pico- or femtosecond) laser pulses when atoms are trapped in a superimposed sequence of two counterpropagating trains of pulses. In analogy with a regular cw FORT, we will call this trap the pulsed FORT. In a pulsed FORT, an atom is not perturbed by the trap laser fields during the time between the optical pulses (for fs optical pulses, one can estimate that the trapped atoms are exposed to the trapping field only 10^{-7}–10^{-6} of the holding time). Hence, such atoms can serve as an ideal object for high-precision spectroscopy, metrology, and experiments on the interaction of atoms with each other and an external field.

The first proposal to use the dipole force resulting from a series of interactions with short counterpropagating laser π-pulses in the area where pulses overlap was made in Ref. [9]. This proposal was confirmed experimentally, first for focusing and deflecting an atomic beam by using picosecond pulses [10] and then in optical trapping of preliminarily cooled ^{85}Rb atoms by using cw and mode-locked lasers (some 10^3 atoms were confined in the trap at $\approx$50 μK) [11]. A comparative experimental study of loading ^{85}Rb atoms from a magneto-optical trap (MOT) to the pulsed and cw FORTs by using a Nd:YAG laser in mode-locked ($\sim$100 ps, 80 MHZ repetition rate) or cw regimes was also reported in Ref. [12]. The laser beam was focused to a waist radius of $\sim$16 μm, which gives for the incident power of $\sim$7 W a potential depth of $\sim$2.1 mK for the cw FORT and 40% lower depth for the pulsed FORT. The authors observed that the pulsed and cw traps behave similarly at the "identical" conditions, but the pulsed trap systematically loaded fewer atoms than the cw one (5% and 8%, respectively). They also found no essential difference in the holding time and the loss rates for one- and two-body collisions between traps. Atomic resonance frequency shift due to the periodic perturbation of the atom in a pulsed FORT, which is different from that in the case of a cw FORT, has been studied both

*yanyshev@physics.msu.ru

theoretically and experimentally, and it was shown that this shift can be eliminated by tuning the pulse energy (the so-called "magic power" concept). This approach has universal applicability, in contrast to the "magic wavelength" concept [13,14].

Theoretical consideration of the pulsed FORTs is essentially based on the well-developed theory of cw FORTs, which largely describes the physics of cold collisions of atoms in optical lattices [15,16]. Specifically in a FORT, in addition to the mechanisms of trapping and simultaneously cooling neutral atoms [2,3,5], one has to take into account the interaction of each single atom with the vacuum modes of the electromagnetic field, which results in the reabsorption of photons emitted into a vacuum field and pairwise dipole-dipole interaction (DDI) between atoms in the ground and excited states, which results from the exchange of spontaneously emitted photons between neighboring atoms [17–21]. The theory of DDI and DDI-based cold collisions was extensively developed for atoms in FORTs [15,16,22–27], including Rydberg atoms [28,29]. Specifically, this theory predicted two-atom cold collisions that, in the presence of an external near-resonant light, are also called light-assisted collisions [27,30–32], which were confirmed and analyzed experimentally [33–35].

Pulsed FORT formed by a superimposed train of femtosecond pulses was first proposed by Balykin, who analyzed the stochastic behavior of a trapped atom by considering a simple model [36]. He demonstrated that it is possible to avoid the stochastic behavior of the trapped atom within a wide range of conditions imposed on the parameters of the femtosecond FORT, and despite rather small values of the depth of the femtosecond trap and the very short interaction time of superimposed pulses with the atom (10^{-7}–10^{-6} of the holding time), an atom can be well-localized in the trap and serve for further experiments in the absence of trapping fields. Nevertheless, the problem of instability [37] and quantum chaos with ultracold atoms [38] is one of the hot topics of the dynamics of ultracold atoms in optical lattices [6,39]. Analysis of a single atom's dynamics in a one-dimensional pulsed optical trap (with a laser pulse duration of 10^{-11}–10^{-13} s) was also performed in Ref. [40]. Our preliminary computer simulation results for atomic dynamics in a femtosecond three-dimensional (3D) FORT are outlined in Ref. [41].

Past research on the pulsed FORTs does not include detailed theory (similar to that developed for cw FORTs) of atomic dynamics in the pulsed trap, which would be three-dimensional and would take into account all key features of the atomic dynamics in the trap, namely, interaction of a single atom with the vacuum electromagnetic field, the DDI of two atoms, and interaction of atoms in the trap with external electromagnetic fields (for instance, a near-resonant probe laser field). This paper presents such a detailed semiclassical theory of atomic dynamics in a pulsed FORT, as well as computer simulation results based on this theory for the case of a femtosecond FORT.

The paper is organized as follows. In Sec. II we describe a pulsed FORT formed by superimposed trains of short laser pulses with a pulse duration of down to a few femtoseconds. The physical model of atomic dynamics in the pulsed FORT, for which a stochastic formulation for the dynamics of an open quantum system is used, is presented in Sec. III. The model includes spontaneous decay of each separate atom in the trap, as well as the effects related to the two-atom interaction, among which the prevailing one is the near-resonant DDI due to the exchange of virtual photons between the atoms via the vacuum electromagnetic field in the field of probe laser radiation near-resonant to the atomic transition. The derivation of the DDI between atoms, as well as the relaxation part of the Liouvillian of the system and its laser Liouvillian due to the interaction with the probe laser field, is also presented in this section. It is based on the theory of quantum random processes, which is well-suited for describing open quantum systems. Technical details of this derivation are given in the Appendices. Simple analytical expressions and analysis are given in Sec. IV for both one-atom and two-atom escapes from the trap (light-assisted cold collisions). The details and results of computer simulation of atomic dynamics in a pulsed fs FORT are discussed in Sec. V using Rb atoms as an example. The power of the fs laser pulse train that forms the trap can be varied to control the depth of the FORT potential and therefore the holding time of the trapped atoms. In computer experiments, we also analyzed the role of the DDI interactions affecting the dynamics of atoms in the FORT under the action of a near-resonant probe laser field. By varying both the intensity and the frequency detuning of the probe field, we modeled the DDI interactions between atoms in short- and long-range limits and analyzed single- and two-atom escape from the trap. In the final section, we summarize our results and discuss some of the possible applications of the femtosecond FORT.

II. MODEL OF THE PULSED FORT

In this work, we analyze the pulsed FORT, which aims to minimize the effect of the localizing field on an atom(s), i.e., we analyze the influence of the short-term and time-periodic action of the laser field on the spatial motion of a very slow atom. In such a scheme, the atom is free of the perturbing effect of the localizing field for a certain time interval $(1-t_p/T)$, where t_p is the duration of the action and T is its repetition period. When femtosecond pulses are used, the relative time interval during which the atom is situated in the localizing field may be very short, i.e., 10^{-7}–10^{-6} of the total time interval during which the atom is confined in the trap. As was shown earlier [36], this approach provides a situation wherein the atom is subjected to the localizing field for only $(10^{-8}$–$10^{-9})\%$ of the total time of its localization; i.e., the atom is almost free (unbound).

The behavior of the particle under the action of a periodic short pulsed force has been actively studied in connection with the problem of classical and quantum chaos [37,38]. Analytical estimates in Ref. [36] and computer simulation results presented therein show that, under certain (experimentally realizable) conditions, it is possible to avoid chaos in the motion of an atom and to achieve its long-term spatial localization.

The basic idea of atomic localization by a periodic sequence of short laser pulses first proposed in Ref. [9] is as follows. Laser pulses are retroreflected from a mirror [Fig. 1(a)]. The incident and reflected pulses "collide" at a certain distance from the mirror. The energy of a single femtosecond pulse is spatially localized at a scale of $l = c/t_p$, where c is the

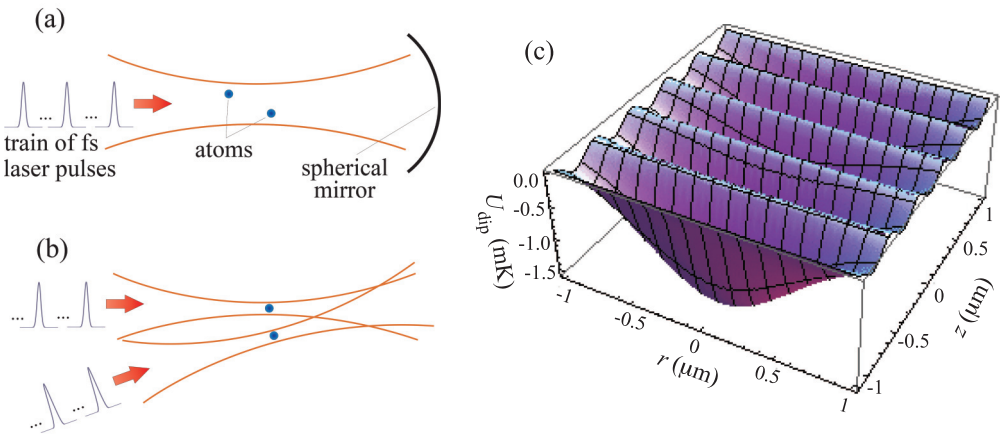

FIG. 1. (Color online) (a) Configuration of the pulsed FORT formed by a train of fs laser pulses. Two atoms, which are confined in the trap and that could be used for studying the interactions between them, are shown in the figure. (b) Another setup for studying the interaction between two closely spaced atoms, each of which is confined in a separate pulsed FORT formed by a train of fs laser pulses (femtotweezers). Interatomic distance can be varied by changing the distance between the femtotweezers. (c) Pulsed FORT potential resulting from interference of the incoming laser pulses and reflected from the mirror laser pulses in configuration (a).

speed of light and t_p is the pulse duration. When the duration of the laser pulse is extremely short, i.e., equal to the period of light [42], its spatial size is equal to the laser wavelength: $l = \lambda$. The region where pulses collide has the same size and is the localization region for the atom. Depending on the phase relations between the incident and reflected pulses, either a maximum or minimum of the laser-field intensity is attained at the center of the overlapping pulses due to their interference. When the laser frequency is lower than the atomic transition frequency and intensity is maximal, an atom placed in the region of the pulse collision is subjected to the gradient force of light pressure that is directed toward the center of the pulse-overlapping region. For rather long fs pulses (100 fs), one can introduce an effective potential of the trap, which is similar to that of a cw FORT [3,5]. However, even when very short, few-cycle light pulses are used, several minima of the potential energy arise [Fig. 1(c)]. After the action of a light pulse, the atom freely moves with a velocity determined by its initial velocity and the momentum gained from the laser field.

For a pulsed FORT formed by retroreflecting a Gaussian laser beam that consists of a train of laser pulses, the wavelength of which is tuned far below the atomic resonance frequency, the spatial intensity distribution of such a focused beam with power P and wave vector k can be written as

$$I(r,z) = \frac{2P}{\pi w^2(z)} \exp\left(-2\frac{r^2}{w^2(z)}\right) \cos^2(kz),$$

where r is the radial coordinate and the $1/e^2$ radius $w(z)$ depends on the axial coordinate z as

$$w(z) = w_0\sqrt{1+\left(\frac{z}{z_R}\right)^2}.$$

Here w_0 is the beam waist radius and $z_R = \pi {w_0}^2/\lambda$ is the Rayleigh length.

Assuming linear polarization of the trap laser field and in the dressed atomic levels picture, the dipole trap potential for a simple two-level atom at the position $\mathbf{r} = (r,z)$ takes the form [5]

$$U_{dip}(\mathbf{r}) = \frac{3\pi c^2\gamma_0}{2{\omega_0}^3} I(\mathbf{r}), \tag{1}$$

where γ_0 is the spontaneous decay rate of the atomic excited state. This formula can also be extended to the case of alkali-metal atoms, which are the major players in the experiments with cold atoms. These atoms feature closed optical transitions lying in a convenient spectral range, so that, e.g., for ^{87}Rb, ^{23}Na, ^{7}Li, and ^{39,41}K, this results in a well-known D line doublet $^2S_{12} \rightarrow {}^2P_{1/2},{}^2P_{3/2}$. Neglecting the hyperfine splitting of the levels, Eq. (1) extends to

$$U_{dip}(\mathbf{r}) = \frac{\pi c^2\gamma_0}{2{\omega_0}^3}\left(\frac{2}{\Delta_2}+\frac{1}{\Delta_1}\right) I(\mathbf{r}), \tag{2}$$

where Δ_1 and Δ_2 are the frequency detunings of the laser radiation from the frequencies of the atomic transitions $^2S_{1/2}\leftrightarrow{}^2P_{1/2}$ and $^2S_{1/2}\leftrightarrow{}^2P_{3/2}$, respectively, and ω_0 is the resonance atomic transition frequency [5].

When an additional near-resonant probe laser field is introduced, it modifies the potential of the trap due to a redistribution of population from the ground energy level of the trapped atoms. As a result, the optical potential becomes

$$U_{dip}(\mathbf{r}) = \frac{(n_1-n_2)\pi c^2\gamma_0}{2{\omega_0}^3}\left(\frac{2}{\Delta_2}+\frac{1}{\Delta_1}\right) I(\mathbf{r}), \tag{3}$$

where

$$n_1 - n_2 = 1 - \frac{2\tilde{g}_L^2}{\left(1+\tilde{\delta_L}^2+2\tilde{g}_L^2\right)}$$

is the population difference between the ground and excited levels, and $\tilde{\delta_L} = \Delta/\gamma_0$ and $\tilde{g_L} = \Omega_R/\gamma_0 = dE/\hbar\gamma_0$ are the dimensionless frequency detuning and the Rabi frequency of the near-resonant probe laser field, respectively [5].

One of the key characteristics of the spatial atomic dynamics in the trap is the lifetime (or escape time) of the atoms in the trap [43]. A single atom localized in a micropotential well of the trap may escape from the well as a result of either

heating due to the optical excitation or collisions with the residual gas. We will not consider the latter mechanism in our work as it is not of fundamental character and, in principle, it can be eliminated in the experiment. At the same time, the interaction of atoms in the trap with an electromagnetic field is a fundamental process and needs to be considered in detail. Simple estimates show that far-detuned from the atomic resonance, laser field of the pump laser beam gives an extremely low probability of absorbing and emitting photons. However, the application of a near-resonant probe laser field allows us to drastically enhance this rate, which significantly affects the atomic dynamics in the trap [27].

In the case of several atoms localized in the trap, we need to consider the laser cooling, heating, the radiative atomic decay, and the near-resonant DDI between pairs of atoms. In this case, when two atoms are localized in the same potential well, their escape could be the result of a short-range DDI or the so-called light-assisted cold collisions between two closely spaced atoms [15].

In this work, we will study the dynamics of a single atom and that of two closely spaced atoms confined in a pulsed (femtosecond) FORT. The latter situation can be realized by placing atoms in the same or adjacent potential well(s) of the FORT potential [Fig. 1(a)]. Alternatively, one can confine atoms in separate FORTs formed by the trains of femtosecond optical pulses, the so-called "femtotweezers" [Fig. 1(b)]. The distance between atoms can then be varied by changing the distance between the femtotweezers. There is not much difference, except for the experimental aspects of their realization, between these two schemes, so that in the following we will consider only the first scheme [Fig. 1(a)].

The parameters of the optical dipole trap used in our model for numerical simulations throughout the paper were taken similar to the parameters used in Ref. [36]. Specifically, we studied the dynamics of Rb atom(s) cooled to a temperature of about 155 nK and confined in the femtosecond red-detuned FORT, which is formed by a laser beam focused to $a \sim 10\,\mu$m from a pulsed laser with a pulse duration of 100 fs operating at 850 nm in the configuration shown in Fig. 1(a).

III. PHYSICAL MODEL OF ATOMIC DYNAMICS IN A PULSED FORT

Under the assumption that atoms in a pulsed FORT interact with the classical electromagnetic field, the evolution of an atom in a trap is governed by the master equation of the general form for the density matrix ρ of an atom,

$$i\hbar\frac{d\rho}{dt} = [H_{\rm A},\rho] + \mathcal{L}\rho, \tag{4}$$

where $H_{\rm A}$ is the atomic Hamiltonian and $\mathcal{L} = \mathcal{L}_{\rm rel} + \mathcal{L}_{\rm L}$ is the total Liouvillian that is the sum of the relaxation and the laser Liouvillians. The relaxation Liouvillian $\mathcal{L}_{\rm rel}$ describes the damping part, i.e., spontaneous decay of the atom due to its interaction with the reservoir in thermal equilibrium with the mean number of photons equal to zero [23] and interaction of two atoms via exchange of virtual photons, i.e., via the DDI. Laser Liouvillian $\mathcal{L}_{\rm L}$ describes the contribution to the total Liouvillian due to the unperturbed dynamics of the atom (free precession with the probe laser frequency $\omega_{\rm L}$). These Liouvillians are derived in Appendices C and D, respectively.

It is extremely difficult and in most cases even impossible to find an exact analytical solution of master equation (4). This leads to possible approximations that allow analytical solutions, or combining analytics with numerical solutions.

In this work, the stochastic formulation of the dynamics of an atom in a pulsed FORT, which is an open quantum system, conveniently allows us to replace master equation (4) with the Langevin-type stochastic differential equation governing the atomic dynamics in the FORT:

$$m\ddot{\mathbf{r}}_i = -\nabla U_{\rm dip}(\mathbf{r}_i) + \mathbf{F}_i(\mathbf{r}_i,t) + \sum_j^N \mathbf{F}_{i,j}(\mathbf{r}_{i,j},t), \tag{5}$$

where m is the atomic mass, index i enumerates the trapped atoms in the trap (up to N), $U_{\rm dip}$ is the dipole trap potential [see Eq. (3)], and $\mathbf{F}_i$, $\mathbf{F}_{i,j}$ are the radiation fluctuation forces acting on a single atom due to the interaction with the vacuum electromagnetic field and due to the pairwise (with the jth atom) DDI, respectively. To solve such a stochastic differential equation, we need to know the radiation fluctuation forces, which are retrieved in this section, and then apply Monte Carlo simulation to Eq. (5).

Over the past two decades, various stochastic formulations of the dynamics of open quantum systems were mainly in the field of quantum optics and in the context of the quantum measurement problem [44,45]. In such a formulation, all processes of atoms–vacuum-field and atoms–near-resonant-laser-field interaction are considered in the Markov approximation, and it is assumed that the fluctuation force $\hat{\mathbf{F}}$ acting on atom(s) due to the interaction with the vacuum and near-resonant probe electromagnetic fields can be treated as an external white noise. We also limit our consideration to the case of a small number of atoms in the trap, so that various collective effects are ignored.

Under these assumptions, the fluctuation force $\hat{\mathbf{F}}$ acting on atom(s) can be described in terms of the correlation function $G_{\mu\nu}(\tau)$ for two atoms at the points $\hat{\mathbf{R}}_\mu$,$\hat{\mathbf{R}}_\nu$ in space:

$$G_{\mu\nu}(\tau) = \langle\hat{\mathbf{F}}(\hat{\mathbf{R}}_\mu,0)\hat{\mathbf{F}}^{\rm T}(\hat{\mathbf{R}}_\nu,\tau)\rangle, \tag{6}$$

where the angle brackets denote averaging over both the field and the internal atomic fluctuations. Superscript "T" in the definition of the correlation function denotes vector transposition that transforms the vector's column $\hat{\mathbf{F}}$ into the corresponding row, so that $G_{\mu\nu}$ for fixed values of μ, ν is a 3×3 matrix.

In the diffusion approximation for the Markov process describing the translational atomic dynamics in the FORT and taking into account the space delocalization of the atomic dipole moment, Eq. (6) can be recast in the form

$$G_{\mu\nu}(\tau) = \int\int\left\langle\frac{\partial}{\partial\mathbf{R}_\mu}\hat{\mathbf{d}}^{\rm T}(\mathbf{r}-\hat{\mathbf{R}}_\mu,0)D(\mathbf{r}-\mathbf{r}',\tau)\times\frac{\partial}{\partial\mathbf{R}_\nu^{\rm T}}\hat{\mathbf{d}}(\mathbf{r}'-\hat{\mathbf{R}}_\nu,\tau)\right\rangle d\mathbf{r}\,d\mathbf{r}', \tag{7}$$

where $D(\mathbf{r}-\mathbf{r}',\tau) = \langle\hat{\mathbf{E}}(\mathbf{r},0)\hat{\mathbf{E}}^{\rm T}(\mathbf{r}',\tau)\rangle$ and $\hat{\mathbf{d}}$ is the atomic dipole moment operator.

As the next step, we will take into account translational fluctuations due to the exchange of photons with the vacuum

electromagnetic field by individual atoms and exchange of virtual photons in between two atoms (interaction via the DDI) in Eq. (7). In the dipole approximation, the corresponding fluctuation force has the form

$$\hat{\mathbf{F}}_{\mathrm{d}} = \int \sqrt{\frac{\hbar\omega}{4\pi^2}} \sum_{\lambda} \hat{\mathbf{d}}(t)\cdot\mathbf{e}_{\lambda}(\mathbf{k})[\hat{a}_{\lambda}(\mathbf{k})\exp(i\mathbf{k}\hat{\mathbf{R}}_{\tau} - i\omega t) - \mathrm{H.c.}]i\mathbf{k}\,d\mathbf{k}, \tag{8}$$

where $\hat{a}_{\lambda}(\mathbf{k})$ are the photon annihilation operators and $\mathbf{e}_{\lambda}(\mathbf{k})$ are their polarization vectors. Then, assuming interaction with the reservoir in thermal equilibrium with the mean number of photons equal to zero [23] and using the approximation $\hat{\mathbf{R}}_{\tau} = \hat{\mathbf{R}}_0 + \hat{\mathbf{v}}\tau$ for the translational motion of atoms, the expression governing the correlation matrix (7) takes the form

$$G_{\mu\nu}(\tau) = \sum_{s} \mathcal{K}_s(\tau) \int \frac{\hbar\omega}{4\pi^2}\mathbf{d}^{\mu}_{\perp s}\cdot\mathbf{d}^{\nu}_{\perp s}\exp\left[i\omega\tau - \delta_{\mu\nu}\frac{\hbar k^2}{2m}\tau - i\mathbf{k}(\hat{\mathbf{R}}_{\nu\mu} + \hat{\mathbf{v}}_{\nu\mu}\tau)\right]\mathbf{k}\mathbf{k}^{\mathrm{T}}d\mathbf{k}, \tag{9}$$

where $\hat{\mathbf{v}}$ is the atom velocity operator, $\hat{\mathbf{d}}_{\perp}$ is the transverse projection of the atomic dipole moment onto the wave vector $\mathbf{k}$, and $\mathcal{K}_s(\tau) \sim \langle\sigma^{-}_{s\mu}(\tau)\sigma^{+}_{s\nu}(\tau)\rangle$ is the correlation function of the sth atomic transition operator. Factor $\delta_{\mu\nu}$ in Eq. (9) determines that the interaction between two different atoms occurs via exchange of virtual photons without energy loss.

Then, the corresponding power spectral density of the correlation function (9) can be written as

$$N_{\mu\nu}(\tilde{\omega}) = \int \sum_{s} S_s\left[\omega - \mathbf{k}\hat{\mathbf{v}}_{\nu\mu} - \delta_{\mu\nu}\frac{\hbar k^2}{2m} + \tilde{\omega}\right]\frac{\hbar\omega}{4\pi^2}\mathbf{d}^{\mu}_{\perp s}\cdot\mathbf{d}^{\nu}_{\perp s}\exp(-i\mathbf{k}\hat{\mathbf{R}}_{\nu\mu})\mathbf{k}k^{\mathrm{T}}d\mathbf{k}, \tag{10}$$

where the matrix function S_s is the Fourier transform of the internal atomic correlation function $\mathcal{K}_s(\tau)$ in Eq. (9). The correlation function $\mathcal{K}_s(\tau)$ can be calculated by using the relaxation superoperator, which is derived in Appendix C. Note that in these calculations one has to subtract the nonfluctuating coherent spectrum contribution, which means that the atomic transition operators are to be biased at their average values:

$$\hat{\sigma}^{\pm}_{\mu} \to \Delta\hat{\sigma}^{\pm}_{\mu} = \hat{\sigma}^{\pm}_{\mu} - \langle\hat{\sigma}^{\pm}_{\mu}\rangle.$$

Further mathematical details of the calculations of the correlation function of the fluctuation force acting on a single atom and on two interacting atoms via the DDI are provided in Appendices A and B. Below, we outline the results that were used in our computer simulations. In the following, we will also enumerate two interacting atoms with indices "1" and "2," so that the random force acting on them is $\hat{\mathbf{F}}_{12}$. For the case of a single atom, we designate it with the index "1" and denote the respective random force acting on it as $\hat{\mathbf{F}}_{11}$.

Then, as follows from Appendices A and B, the spectral matrix for the random radiative force $\hat{\mathbf{F}}_{11}$ acting on a single atom in a pulsed FORT is

$$N_{11} = \frac{\hbar\omega_0^5 d^2}{2\pi c^5}\langle\Delta\sigma_1^{-}\Delta\sigma_1^{+}\rangle I_{11}, \tag{11}$$

where I_{11} is the dimensionless 3×3 matrix, $d = (3\hbar c^3\gamma_0/4\omega_0^3)^{1/2}$ is the atomic transition dipole moment, γ_0 is the decay rate of the atomic transition, ω_0 is the atomic transition frequency, and $\hat{\sigma}^{\pm}$ are the atomic transition operators.

For two atoms in a pulsed FORT interacting via the DDI, the respective spectral matrix for the random radiative force $\hat{\mathbf{F}}_{12}$ acting on both atoms in the trap is equal, as follows from Appendix B, to

$$N_{12} = N_{21} = \frac{\hbar\omega_0^5 d^2}{2\pi c^5}\langle\Delta\sigma_1^{-}\Delta\sigma_2^{+}\rangle I_{12}, \tag{12}$$

where I_{12} is the dimensionless 3×3 matrix, which is determined by the geometry of the atomic dipole moments with respect to the vector of atomic displacement and to the wave vector of the emitted photon.

For the case of the atomic dipole moments parallel to each other and orthogonal to the vector of displacement between the atoms, i.e.,

$$\mathbf{d}^1_{\perp} \parallel \mathbf{d}^2_{\perp} \perp \mathbf{R}_{12}, \tag{13}$$

we have (see Appendix B)

$$I_{11} = \pi\begin{pmatrix} \frac{8}{15} & 0 & 0 \\ 0 & \frac{16}{15} & 0 \\ 0 & 0 & \frac{16}{15} \end{pmatrix}, \quad I_{12} = \pi\begin{pmatrix} \tilde{I}_1 & 0 & 0 \\ 0 & \tilde{I}_2 & 0 \\ 0 & 0 & \tilde{I}_3 \end{pmatrix}, \tag{14}$$

where

$$\begin{aligned} \tilde{I}_1 &= \frac{4\left(9-\varphi_{12}^2\right)\cos\varphi_{12}}{\varphi_{12}^4} - \frac{4\left(9-4\varphi_{12}^2\right)\sin\varphi_{12}}{\varphi_{12}^5}, \\ \tilde{I}_2 &= \frac{4\left(3-\varphi_{12}^2\right)\cos\varphi_{12}}{\varphi_{12}^4} - \frac{4\left(3-2\varphi_{12}^2\right)\sin\varphi_{12}}{\varphi_{12}^5}, \\ \tilde{I}_3 &= \frac{-4\left(12-3\varphi_{12}^2\right)\cos\varphi_{12}}{\varphi_{12}^4} + \frac{4\left(12-7\varphi_{12}^2+\varphi_{12}^4\right)\sin\varphi_{12}}{\varphi_{12}^5} \end{aligned} \tag{15}$$

and $\varphi_{12} = R_{12}(\omega_0/c)$ is the dimensionless interatomic distance.

In the case of a single atom, i.e., at $R_{12}\to 0$, Eqs. (15) simplify to

$$\tilde{I}_2 = \tilde{I}_3 = 2\tilde{I}_1 = \tfrac{16}{15}, \tag{16}$$

i.e., they yield the same value as the one that can be obtained by direct integration for a single atom. Note also that fluctuations along the direction of the dipole moment are two times weaker than in the orthogonal directions.

In the limit of long-range interactions, i.e., at $R_{12} \gg \lambda$, we have

$$\tilde{I}_1 = \tilde{I}_2 = 0, \quad \tilde{I}_3 = \frac{4\sin\varphi_{\mu\nu}}{\varphi_{\mu\nu}}, \tag{17}$$

which means that the long-range fluctuations are the ones along the interatomic distance.

In Eqs. (11) and (12), $\langle\Delta\sigma_1{}^{-}\Delta\sigma_2{}^{+}\rangle$ is the correlation function of the operator of exchanging photons between two

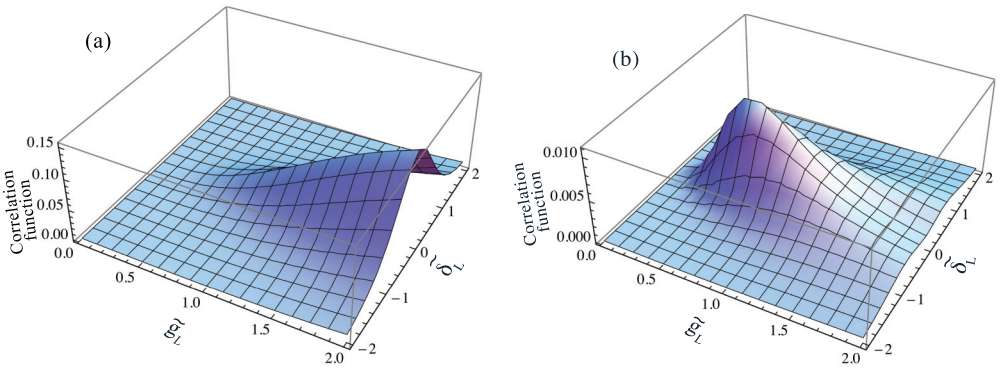

FIG. 2. (Color online) Correlation functions $\langle \Delta\sigma_1^- \Delta\sigma_1^+ \rangle$ (a) and $\langle \Delta\sigma_1^- \Delta\sigma_2^+ \rangle$ (b) vs the dimensionless Rabi frequency $\tilde{g}_L$ and the frequency detuning $\tilde{\delta}_L$ of the probe laser field.

atoms [Fig. 2(b)], which reads

$$\langle \Delta\sigma_1^- \Delta\sigma_2^+ \rangle = \frac{-4\zeta \tilde{g}_L^4 \left(1 + 4\tilde{\delta}_L^2\right)}{\left[(1+\zeta)^2 + 4\left(\tilde{g}_L^2 + \tilde{\delta}_L^2\right) + 4(1+\zeta)^2\tilde{\delta}_L^2 + 4\left(\tilde{g}_L^2 + 2\tilde{\delta}_L^2\right)^2\right]^2}, \tag{18}$$

where $\tilde{g}_L = g_L/\gamma_0$ ($g_L = Ed/\hbar$) and $\tilde{\delta}_L = \Delta/\gamma_0$ are the dimensionless Rabi frequency and frequency detuning of the probe laser field, respectively, and

$$\zeta = \frac{3}{2} \frac{\varphi \cos\varphi - \sin\varphi + \varphi^2 \sin\varphi}{\varphi^3} \tag{19}$$

is the dimensionless geometrical factor, which in the limit of the long-range interactions, i.e., at $R_{12} \gg \lambda$, simplifies to [see Eq. (C5)]

$$\zeta = 3 \sin\varphi / 2\varphi. \tag{20}$$

For closely spaced atoms, at $R_{12} \to 0$, Eq. (19) yields $\zeta = 1$, which corresponds to total correlation of stationary excitations. The case of antiparallel dipole moments $\mathbf{d}_\mu, \mathbf{d}_\nu$ corresponds to another limiting value $\zeta = -1$. It is worth noting that the combination of Eqs. (14) and (20) yields an inverse square dependence on the interatomic distance with a positive sign of the ζI factor.

Then, assuming that $\zeta = 1$ in the limit for a single atom, one can calculate the correlation function of the fluctuations of a single atom [Fig. 2(a)], which has the form

$$\langle \Delta\sigma_1^- \Delta\sigma_1^+ \rangle = \frac{2\tilde{g}_L^4 \left[1 + 2\left(\tilde{g}_L^2 + \tilde{\delta}_L^2\right)^2 + \left(1 + 4\tilde{\delta}_L^2\right)\right]}{\left[4 + 4\left(\tilde{g}_L^2 + \tilde{\delta}_L^2\right) + 16\tilde{\delta}_L^2 + 4\left(\tilde{g}_L^2 + 2\tilde{\delta}_L^2\right)^2\right]^2}. \tag{21}$$

The correlation function of the operator of exchanging virtual photons between two atoms $\langle \Delta\sigma_1^- \Delta\sigma_2^+ \rangle$, which describes the DDI between atoms, reaches its maximum at detuning $\tilde{\delta}_L = -1$ when the interaction force between atoms has its maximum value with respect to fluctuations of the random radiation force acting on a single atom. This maximum is reached at $\tilde{g}_L = 1.4$, which corresponds to the probe laser field intensity $I = 3.14\ \mathrm{mW/cm^2}$.

It is also worth calculating the so called normalized correlation coefficient, or simply the DDI efficacy (see Fig. 3),

$$\kappa = \frac{N_{12}}{N_{11}} = \frac{-2\zeta\left(1 + 4\tilde{\delta}_L^2\right)}{A_3}, \tag{22}$$

where

$$N_{11} \propto \langle \Delta\sigma_\mu^- \Delta\sigma_\mu^+ \rangle = \frac{2\tilde{g}_L^4 A_3}{A_0^2},$$

$$A_3 = \left[1 + 2\left(\tilde{g}_L^2 + 2\tilde{\delta}_L^2\right)\right]^2 + \zeta^2\left(1 + 4\tilde{\delta}_L^2\right).$$

It follows from Eq. (22) that the correlation effects are most vividly observed in the weak field limit, at $\mathbf{E}_L\mathbf{d}/\hbar \ll \gamma_0$, i.e., at the extreme values of $\kappa = \mp 1$, which correspond to $\zeta = \pm 1$ and $\tilde{\delta}_L = 0$.

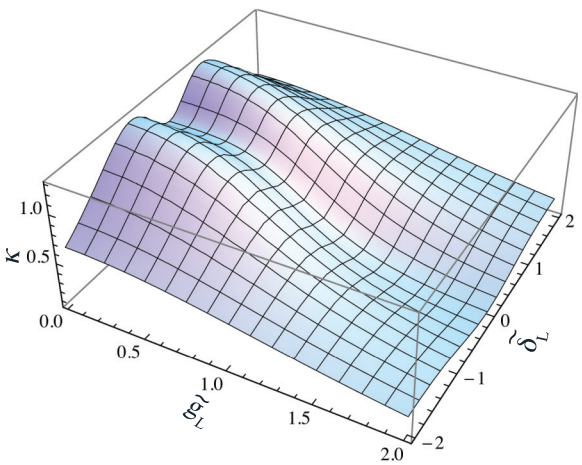

FIG. 3. (Color online) The DDI efficacy κ vs the dimensionless Rabi frequency $\tilde{g}_L$ and the frequency detuning $\tilde{\delta}_L$ of the probe laser field.

IV. ANALYSIS OF ONE- AND TWO-ATOM ESCAPES FROM THE TRAP

In this section, we will perform a simplified analysis of the atom escapes from the FORT. In the stochastic formulation of the dynamics of atoms in a pulsed FORT outlined in Sec. III, the events of escape of one atom or several atoms simultaneously from the FORT (we will limit our consideration to two-atom escapes because the probability of multiple-atom escape from the trap is negligibly low) can be described by the stationary correlation matrix $K_{\mu\nu} = \langle \hat{\mathbf{R}}_\mu, \hat{\mathbf{R}}_\nu \rangle$, which, similarly to Sec. III, has the form

$$K_{\mu\nu} = \frac{2\pi^2 N_{\mu\nu}}{m^2\Gamma^3}[\lambda_+\lambda_-(\lambda_+ + \lambda_-)]^{-1},$$
$$\lambda_\pm = \frac{1}{\sqrt{2}}\left[1 - \frac{\varepsilon}{2} \pm \sqrt{\left(1 - \frac{\varepsilon}{2}\right)^2 - \frac{\varepsilon^2}{4}}\right]^{-1}, \quad \varepsilon = \frac{4\omega^2}{\Gamma^2}, \tag{23}$$

where we assume that, as in Ref. [5], the damping rate Γ due to the damping forces acting on an atom in the FORT is

$$\Gamma = \frac{4\pi\hbar\omega^2}{mc^2}\,\frac{\tilde{g}_{\mathrm{L}}^2}{\tilde{g}_{\mathrm{L}}^2 + \tilde{\delta}_{\mathrm{L}}^2 + 2}\,\frac{-\tilde{\delta}_{\mathrm{L}}}{\left(1 + \tilde{\delta}_{\mathrm{L}}^2\right)^2}$$

and the temperature of atoms in the trap can be estimated as $T = N_{11}/(k_B m\Gamma)$; $N_{\mu\nu}$ is the power spectral density of the fluctuation force due to the emission radiation [see Eq. (10)], and we also assume that a nonperiodic behavior at $\varepsilon < 1$ plays a major role [46].

Integration of the probability density $f(p)$ over space, $|x_1| > a, \ldots, |x_n| > a$, where a is the size of the trap, yields a probability $\mathcal{P}_n$ of escape of n atoms out of N trapped atoms, which is represented by the ket-vector x of their momenta and $x^{\mathrm{T}} = (x_1, \ldots, x_N)$ is the corresponding bra-vector. Under the assumption of the Gaussian character of the fluctuations, the probability density is given then by the function

$$f(p) = \det{}^{-1/2}(2\pi K)\exp\left(-\tfrac{1}{2}x^{\mathrm{T}}K^{-1}x\right). \tag{24}$$

In the case of $\hat{\mathbf{R}}_\mu, \hat{\mathbf{R}}_\nu \ll a$ and using a linear local approximation of the Gaussian exponential in Eq. (24), we have

$$\mathcal{P}_n = \frac{\det{}^{-1/2}(2\pi K_n)}{a^n}\exp\left[-\frac{a^2}{2}\sum_{kj}(-1)^{\nu_j+\nu_k}\left|K_n^{-1}(j,k)\right|\right]$$
$$\times\left[\prod_{k=1}^{n}\sum_j\left|(-1)^{\nu_j+\nu_k}K_n^{-1}(j,k)\right|\right]^{-1} \tag{25}$$

for the probability of n atoms escaping simultaneously from the trap, with different signs in the limit $\hat{\mathbf{R}}_k > a$ or $\hat{\mathbf{R}}_k < -a$, depending on the ν_k in $(-1)^{\nu_k}$. Here K_n^{-1} is the $n \times n$ submatrix of the total $N \times N$ inverse correlation matrix K^{-1}.

For simplicity, let us consider the case of an atomic ensemble that consists of just two equivalent atoms, i.e., $N = 2$. In this case, the spectral density matrix has only two independent matrix elements $N_{12} = \kappa N_{11}$, where κ is the DDI efficacy. Then, in accordance with Eq. (23) we have two independent correlation matrix elements, K_{11} and K_{12}. In this case, the probabilities (25) for $n = 1,2$ are determined then by three independent probabilities, which are as follows:

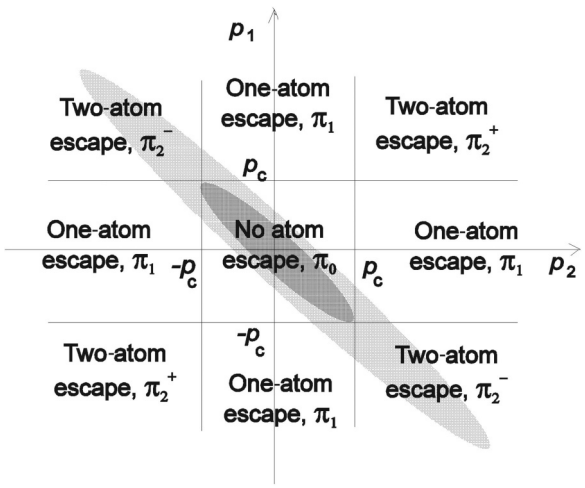

FIG. 4. Integration of the probability density over the domains of atomic escape for two trapped atoms. The probability distribution is shown as a gray-scale-map graph and corresponds to $\kappa \approx -1$. Out-of-the-center areas at the corners on the plot show probabilities $\pi_2^\pm$ at which both atoms escape together from the trap having either positive or negative momenta (indicated by the respective superscript sign of the probability). The rest of the out-of-center areas show probability $\pi_1^\pm$ at which only one atom escapes from the trap. The central area corresponds to the case when no one atom escapes from the trap.

(i) $\pi_1 = \mathcal{P}(x_1 > a)$ is the probability for one of the atoms to escape with positive momentum, while the second atom remains in the trap.

(ii) $\pi_2^- = \mathcal{P}(x_2 < -a)$ is the probability for both atoms to escape together, one having positive and the other one having negative momentum.

(iii) $\pi_2^+ = \mathcal{P}(x_2 < -x_c)$ is the probability for both atoms to escape together, each having a positive momentum.

Other escape probabilities coincide with those listed above, as shown in Fig. 4. Also, the probability for the atoms not to escape and remain captured in the trap is equal to $\pi_0 = 1 - 4\pi_1 - 2(\pi_2^- + \pi_2^+)$.

To analyze the atomic escape probabilities, let us introduce the so called escape variables $\varepsilon_k = -1,0,1$ for the kth atom. The escape variable $\varepsilon_k = -1$ corresponds to the escape of the kth atom from the trap with negative momentum, $\varepsilon_k = 0$ corresponds to the case when the kth atom remains in the trap (no escape), and $\varepsilon_k = +1$ corresponds to the case when the kth atom escapes from the trap with positive momentum. Then, the joint probability can be represented by the corresponding matrix:

$$\mathcal{P}(\varepsilon_1,\varepsilon_2) \to P = \begin{pmatrix} \pi_2^- & \pi_1 & \pi_2^+ \\ \pi_1 & \pi_0 & \pi_1 \\ \pi_2^+ & \pi_1 & \pi_2^- \end{pmatrix}. \tag{26}$$

Then, one can express the probabilities π_1, π_2^+, and π_2^- in terms of the correlation matrix K:

$$\pi_1 = \sqrt{\frac{K_{11}}{2\pi a^2}}\exp\left(-\frac{a^2}{2K_{11}}\right),$$
$$\pi_2^\pm = \frac{K_{11}}{2\pi a^2}\sqrt{\frac{1 \pm \kappa}{1 \mp \kappa}}\exp\left[-\frac{a^2}{K_{11}(1 \pm \kappa)}\right]. \tag{27}$$

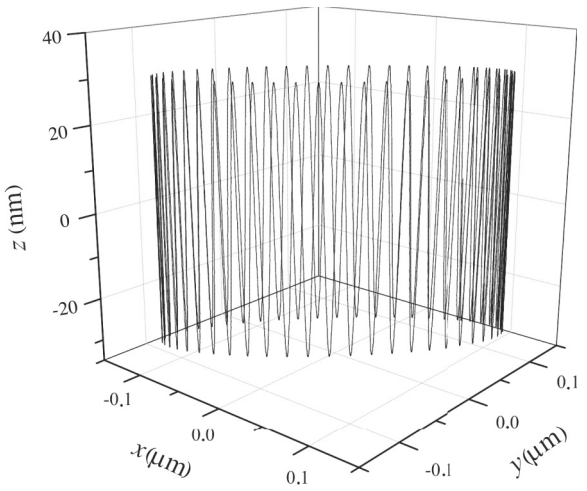

FIG. 5. A sample trajectory of a Rb atom confined in a femtotrap. The depth of the trap potential is equal to 1 mK, and the probe near-resonant laser is switched off.

Evidently, in the absence of correlations between atoms, we should simply have $P_2 = 2P_1^2$, where $P_2 = 2\pi_2^- + 2\pi_2^+$ and $P_1 = 2(\pi_1 + \pi_2^- + \pi_2^+)$ are the total probabilities of two-atom and single-atom escapes, respectively. This is equivalent to the simple relation $\pi_2^- = \pi_1^2$, which follows from Eq. (27).

V. COMPUTER MODELING OF ATOMIC DYNAMICS IN A PULSED fs FORT

In this section, we consider computer modeling of atomic dynamics in a pulsed fs FORT, which is based on the Monte Carlo simulation of the Langevin-type stochastic differential equation (5) for the atomic dynamics in the trap. As we demonstrated in Sec. III, in this approach the radiation fluctuation forces acting on atoms can be readily calculated, and analytical formulas for them were derived. In order to simulate these forces on a computer, we model them by independent random forces, the amplitudes of which are generated by a computer random number generator in such a way as to preserve the given level of the mean-square fluctuations of these forces. Specifically, we use the following formula for the mean-square dispersion of the integral of the radiation force acting on an atom during the sampling time Δt:

$$\sigma_{ij}^{\lambda\,2}(\Delta t) = \overline{\left[\int_0^{\Delta t} F_{ij}^{\lambda}(\tau)\,d\tau\right]^2} = N_{ij}^{\lambda}\Delta t, \tag{28}$$

where the indices i,j label the atoms, $F_{i,j}^{\lambda}$ are the projections of the radiation fluctuation force $\mathbf{F}_{i,j}$ on axis, $\lambda = x,y,z$, and $N_{i,j}^{\lambda}$ are the nonzero components of the power spectral density matrix N calculated from Eqs. (11) and (12), which describe the diagonal elements of the 3×3 submatrices of the block-matrix of the form

$$N = \begin{pmatrix} N_{11} & -N_{12} \\ -N_{12} & N_{11} \end{pmatrix}.$$

Projections of forces $F_i^{\lambda} = \sum_j \mathbf{F}_{i,j}$, which satisfy relation (28), can be written as

$$\begin{aligned} F_1^{\lambda} &= \left(\sqrt{12\left|N_{11}^{\lambda} + N_{12}^{\lambda}\right|/\Delta t}\,\xi_1^{\lambda}\right. \\ &\quad \left. - \sqrt{12\left|N_{11}^{\lambda} - N_{12}^{\lambda}\right|/\Delta t}\,\xi_2^{\lambda}\right)/\sqrt{2}, \\ F_2^{\lambda} &= \left(\sqrt{12\left|N_{11}^{\lambda} + N_{12}^{\lambda}\right|/\Delta t}\,\xi_1^{\lambda}\right. \\ &\quad \left. + \sqrt{12\left|N_{11}^{\lambda} - N_{12}^{\lambda}\right|/\Delta t}\,\xi_2^{\lambda}\right)/\sqrt{2}, \end{aligned} \tag{29}$$

where $\xi_{1,2}^{\lambda}$ are independent random variables uniformly distributed in the interval $[-1/2,1/2]$, which can be generated by a regular computer random numbers generator.

In a computer experiment, we studied the dynamics of Rb atom(s) cooled to about 155 nK and confined in a femtotrap, which is formed by a laser beam focused to $a \sim 10$ μm from a pulsed laser with a pulse duration of 100 fs that operates at 850 nm in the configuration shown in Fig. 1(a). As was mentioned above, the dynamics of trapped atoms is governed by the Langevin-type stochastic differential equation (5), which we integrated numerically with a variable time step of the order of 1 fs. This model includes all mechanisms of atomic interaction with the vacuum electromagnetic field (pairwise DDI interaction inclusive), as well as interaction with the probe near-resonant laser field, which is described in detail in Sec. III.

In our calculations, we assumed that the pulsed fs FORT is formed by a train of fs pulses with linear polarization. Then, it is also reasonable to assume that the atomic dipole moments

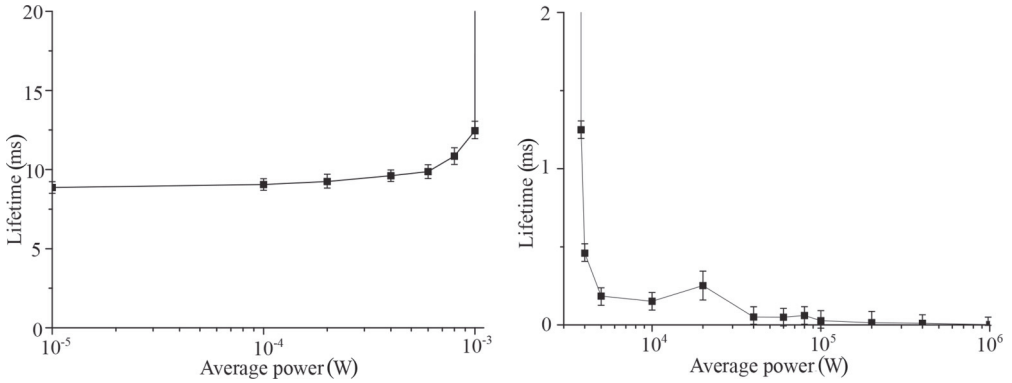

FIG. 6. The lifetime of a Rb atom confined in a femtotrap vs the power (on a logarithmic scale) of the laser beam forming the trap focused to 10 μm (right figure). The left figure shows this dependence at low power values in detail.

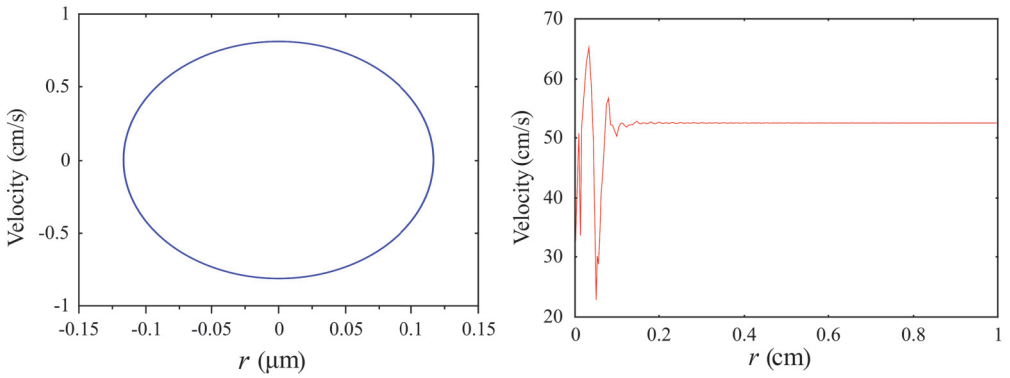

FIG. 7. (Color online) Phase portraits for a Rb atom confined in a femtotrap at two different powers of the laser beam forming the trap: 1 W (left) and 5 kW (right).

of the atoms trapped in the potential wells are parallel to each other and orthogonal to the displacement vector between the atoms, i.e., the geometry condition (13) is fulfilled.

A sample trajectory of a Rb atom confined in the fs FORT is shown in Fig. 5. From this figure, one can clearly see that the atom confined in the femtotrap rapidly oscillates along the z direction of the FORT and makes slow precession along the circle in the plane perpendicular to the beam direction. It is also important to note that the confined atom is tightly localized (within a few dozen nm) in the z direction, whereas localization in the radial direction is about 0.2 μm. In the first approximation, the oscillation frequencies of the trapped atoms are equal to $\omega_r = (4U_0/mw_0^2)^{1/2}$ in the radial direction and $\omega_z = k(2U_0/m)^{1/2}$ in the axial direction, respectively [5].

Let us now examine how the lifetime of the atoms confined in the femtotrap depends on the power of the trap laser beam (Fig. 6). For low power (well below 1 mW) of the laser beam forming the trap, which is too low to confine atoms, the lifetime of atoms in the trap is obviously rather short and is determined by the time it takes for an atom to cross the laser beam, e.g., about 10 ms (Fig. 6, left). It drastically increases with the increase in laser power up to 1 mW. Above this threshold, atoms are confined in the femtotrap for an infinite (under certain conditions) time. However, with further increase in laser power beyond the upper threshold of about 4 kW, the lifetime of the atoms sharply drops. Therefore, our simulations give an optimal range from 1 mW to 4 kW for the power of the laser beam forming the femtotrap to efficiently trap Rb atoms.

Phase portraits for a Rb atom confined in the fs FORT at two different levels of power of the laser beam forming the trap are shown in Fig. 7. They clearly demonstrate two limiting cases: the confinement of an atom in the trap at powers in the optimal range (left figure) and its escape from the trap at powers beyond this range (right figure). A single atom escapes from the trap due to its radiative heating (see Ref. [36] for details).

Now, let us analyze the influence of the DDI on the atomic dynamics in the fs FORT. The model used to describe the DDI, which was always taken into account in our calculations, is outlined in Sec. III. Despite the DDI between the atoms in the trap being rather weak, it can be significantly enhanced by illuminating the atoms by a near-resonant cw probe laser field (for Rb atom, its wavelength lies in the vicinity of 780 nm). Figure 8 shows a sample trajectory and a phase portrait of an atom trapped in the fs FORT, which escapes from the trap due to the action of the resonant probe laser field.

Figure 9 shows the lifetime of the atom trapped in the fs FORT under the action of the near-resonant probe laser field that surely causes the heating of the atom and its radiative escape. This simplified picture becomes more complicated in the 3D case, when we consider a tightly focused laser beam in our calculations, so that the Stark shift of the atomic transition depends on the position of the atom in the beam

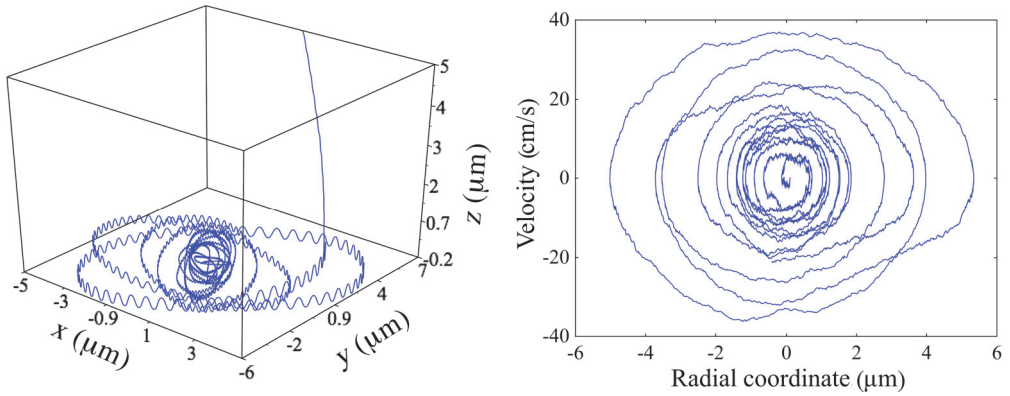

FIG. 8. (Color online) Sample trajectory (left) and phase portrait (right) for a Rb atom confined in the fs FORT under the action of a probe laser field that is near-resonant with the atomic transition with a power of 1 W.

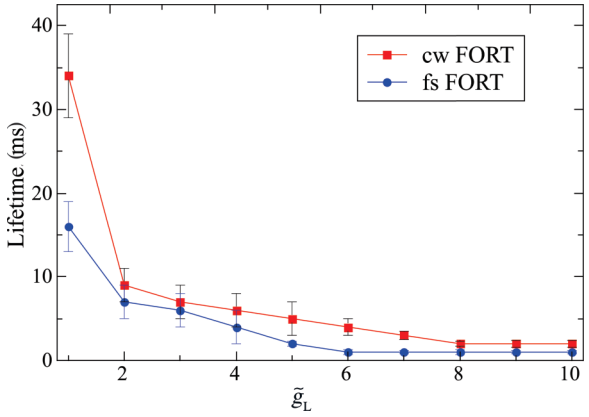

FIG. 9. (Color online) The lifetime of a Rb atom confined in the cw and fs FORTs vs the dimensionless Rabi frequency $\tilde{g}_L$ of the probe laser field, which is tuned in the resonance with the atomic transition ($\tilde{\delta}_L = 0$). The average power of the laser beam forming both traps in our calculations is equal to 1 W.

and changes during the temporal dynamics of an atom in the trap. Keeping in mind that the frequency shift of the probe laser field that is near-resonant with the atomic transition is a constant value, the position-varying Stark shift results in the position-varying heating of the atom as well as the position-varying Doppler cooling force, which are both taken into account in our calculations. For comparison, Fig. 9 shows the lifetime of the atom trapped in a cw FORT that is formed by a cw pump laser of the same power as the average power used for the fs FORT. The comparison of the trapping efficacy of the cw and the pulsed fs FORTs clearly demonstrates that, at low values of the dimensionless Rabi frequencies, the cw FORT outperforms its femtosecond counterpart, but upon increasing the dimensionless Rabi frequency of the probe laser beam, at $\tilde{g}_L \gtrsim 2$, both traps trap the atoms equally well. Note that, in the absence of the probe laser field, the lifetime of an atom in both cw and fs FORTs is infinitely long in our model, provided that there are no collisions with the residual gas, etc.

The dependencies of the lifetime of a single atom and two neighboring atoms trapped in the femtotrap calculated from our computer experiments are shown in Fig. 10. For the experiments with a single atom, one can clearly see that the lifetime is drastically decreased (compare with Fig. 6). The slow decrease in the lifetime upon increasing the distance of the atom from the center of the beam is obviously due to the slow drop of the intensity of the beam forming the trap at the current location of the atom.

In the experiments with two atoms interacting via the DDI, their lifetime in the trap versus the distance between the atoms behaves very differently. As follows from the DDI model (Sec. III), interaction between atoms is most vividly revealed when the atoms are located in the closest micropotentials (first point on the left in the corresponding dependence in Fig. 10) and results in a decrease in the lifetime by a factor of 4.5 times relative to the case of a single atom. This difference is naturally decreased upon increasing the distance between the atoms and, finally, at a distance of 3λ (the second atom is located inside the 10th micropotential from the center of the beam forming the trap), it almost completely coincides with the dependence for a single atom. In Fig. 10, the value of the probe laser beam frequency detuning from the atomic resonance is equal to γ_0, which is the optimal value, as can be seen from Fig. 3, which illustrates the dependence of the DDI efficacy κ on the dimensionless frequency detuning $\tilde{\delta}_L$ of the probe laser field predicted by Eq. (22). On can see from this figure that the peak of the DDI efficacy is reached at the frequency detuning of the probe laser beam nearly equal to γ_0.

VI. CONCLUSION

In conclusion, we presented a detailed semiclassical theory of atomic dynamics in a 3D pulsed optical dipole trap, which

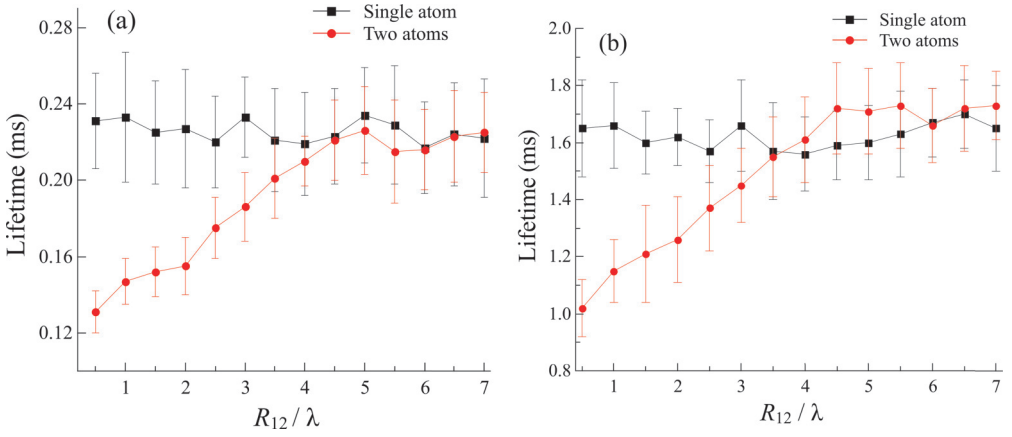

FIG. 10. (Color online) The lifetime of a single atom and two neighboring atoms trapped in a femtotrap. For the pair of atoms, this time is plotted vs the distance R_{12} between the atoms normalized to the wavelength of the formation of the trap laser beam, one of which is located in the center ($x, y, z = 0$) of the focused beam, and the second one is located in the neighboring potential well. For the experiments with a single atom, the holding time is plotted vs the normalized distance between the center of the trap and the potential well in which the atom is located. The train of the femtosecond pulses forming the trap with a power of 1 W is focused on spots with a diameter of 5 μm (a) and 1 μm (b), respectively. The intensity of the probe laser beam is equal to $5I_{sat}$, where I_{sat} is the saturation intensity of the atomic transition, and the frequency of the probe field is detuned from the resonance with this transition by $\sim\gamma_0$, which is the decay time of the transition. Each point on the plots is an average over 10 computer realizations.

is formed by a superimposed train of short laser pulses (down to a few fs duration), based on the stochastic formulation of the dynamics of an open quantum system. It covers all key features of the atomic dynamics in the trap, including the DDI between trapped atoms due to the exchange of virtual photons between them. Analytical solutions are obtained for the relaxation and laser Liouvillians that describe the dissipation and laser excitation in the system. The probabilities of a single-atom and two-atom escape from the trap are analyzed.

This theory was applied to computer simulation of the dynamics of Rb atoms preliminarily cooled in a MOT trapped in a femtosecond optical dipole trap (pulse duration 100 fs). The computer simulation proved that such a trap effectively confines atoms at a pump laser beam power between 1 mW and 4 kW. It is shown that an atom can be localized with absolute accuracy in a few tens of nanometers range. The time interval during which the atom remains in the laser field is only 10^{-7}–10^{-8} of the total localization time.

One of the key advantages of the femtosecond FORT is that interaction of trapped atoms with an external field(s) and between each other can take place within the time interval between the fs pulses, i.e., in the absence of any pump field. This makes it feasible to use the femtosecond FORT for high-precision measurements that cannot be arranged otherwise. As an example, we consider a near-resonant DDI through which a single trapped atom or atoms that are closely spaced in the micropotential wells interact. This interaction is negligibly small without an external near-resonant probe field, however it can be drastically enhanced in an experiment by illuminating the atoms with a cw near-resonant to the atomic transition probe laser field. We presented a model for the DDI and our calculations clarified in detail how the DDI enhanced by the near-resonant laser field affects the atomic dynamics in the trap.

The physics of cold collisions between atoms in a FORT can be studied experimentally not only by means of the traditionally used analysis of one- and two-atom losses from the trap, but also using spontaneous fluorescence and resonance fluorescence from the atoms in the trap. As was shown in theory and confirmed experimentally, the system of two two-level or multilevel atoms interacting via the DDI is a source of quantum entanglement [47–49], as well as a source of cooperative effects in atomic fluorescence, which reveal themselves in the form of macroscopic quantum jumps (light and dark periods), both in ions and atoms [50–52]. Moreover, this fluorescence and, therefore, the interaction between the atoms in the trap can be microscopically resolved [53]. In addition, it was shown that analysis of quantum features of the resonance fluorescence from a system of two colliding neutral or ionized atoms with excited states that exhibit fine-structure splitting can reveal the collisional dynamic correlations between the atoms, making resonance fluorescence a sensitive probe of atomic dynamics in the trap [54].

Increasing the number of trapped atoms in an optical lattice also brings new physics into play. For example, for a large ensemble of Rydberg atoms in an optical lattice interacting via the long-range DDI, it is predicted that such a system occasionally exhibits collective quantum jumps between the states with low and high Rydberg populations [39].

ACKNOWLEDGMENTS

We thank Igor Shumay, Jon Sjogren, Ilya Tarakanov, and Maxim Piskunov for their help in preparing this paper. This work was partly supported by the Russian Ministry of Science and Education under Grant No. 8393, by the Russian Foundation for Basic Research under Grant No. 12-02-00784-a, and by the Program "Extreme Light Fields" of the Presidium of the Russian Academy of Sciences.

APPENDIX A: CALCULATION OF THE CORRELATION FUNCTION OF THE FLUCTUATION FORCE ACTING ON A SINGLE ATOM

For a single atom exchanging photons with the vacuum electromagnetic field, Eq. (10) governing the power spectral density of the correlation function (9) versus frequency ω shifted due to the recoil momentum simplifies (with $\mu = \nu$) to

$$N(\tilde{\omega}) = \frac{\hbar}{4\pi^2 c^5} \int \sum_s S_s \left[\omega \left(1 - \frac{\mathbf{n}\hat{v}}{c} - \frac{\hbar\omega}{2mc^2} \right) + \tilde{\omega} \right] \times d_{\perp s}^2 \mathbf{n}\mathbf{n}^{\mathrm{T}} \omega^5 d\omega \, d\mathbf{n}. \quad \text{(A1)}$$

From this equation, one can easily see that the power spectral density of the force fluctuations is given by the integral over frequencies $\tilde{\omega}$ of emitted photons and their directions $\mathbf{n} = \mathbf{k}/k$, where the Doppler shift and the recoil energy are taken into account. For integration over velocities, one can use the Doppler-broadened spectrum $S_{\mathrm{D}s}$ instead of spectrum S_s for a fixed atom, so that, for the case of isotropic Doppler broadening, the fluorescence spectrum takes the form

$$N(\tilde{\omega}) = \frac{2}{15} \frac{\hbar}{\pi c^5} \int_0^\infty \sum_s d_s^2 S_{\mathrm{D}s} \left[\omega \left(1 - \frac{\hbar\omega}{2mc^2} \right) + \tilde{\omega} \right] \times \omega^5 d\omega (P_s^{\parallel} + 2P_s^{\perp}), \quad \text{(A2)}$$

where $P_s^{||}$ and $P_s^{\perp}$ are the projection matrices onto the directions of the dipole moments and the orthogonal planes, respectively.

For simplicity, let us assume now that $S_{\mathrm{D}s}$ can be treated as a narrow spectrum around the central frequency ω_s. To neglect the recoil energy, let us consider only the spectral range with $\tilde{\omega} \ll \omega_s$. Then, using the integral equation $\int S_{\mathrm{D}s} d\omega = 2\pi n_s$, where n_s is the excited-state population of the sth transition, which corresponds to $\tau \to 0$ in the correlation function $\hat{\sigma}_s^- \hat{\sigma}_s^+$, and replacing n_s with $n_s - \langle \hat{\sigma}_s^- \rangle \langle \hat{\sigma}_s^+ \rangle$ in order to get rid of the coherent part of the spectrum, we get finally

$$N(\omega) = \frac{\hbar^2}{5c^2} \sum_s \gamma_s \omega_s^2 (n_s - \langle \hat{\sigma}_s^- \rangle \langle \hat{\sigma}_s^+ \rangle)(P_s^{\parallel} + 2P_s^{\perp}), \quad \text{(A3)}$$

where γ_s is the radiation decay rate of the sth atomic transition.

From this formula, one can easily see that, at low frequencies ($\omega \ll \omega_s$), the power spectral density of the force fluctuations does not depend on frequency and, therefore, ideally mimics the white noise. Also, the spectral density is proportional to the photon emission rate of each atomic transition and has an anisotropic character, i.e., the intensity of the components orthogonal to $\mathbf{d}_s$ exceeds the intensity of the parallel ones by a factor of 2.

APPENDIX B: CALCULATION OF THE CORRELATION FUNCTION OF THE FLUCTUATION FORCE ACTING ON TWO INTERACTING ATOMS

Now, we will describe mathematically the interaction of two atoms via the DDI in the near-resonant probe laser field. For simplicity, we will neglect fluctuation frequencies $\tilde{\omega}$ with respect to frequencies $\sim\omega_{\mathrm{L}}$ of photons emitted by the atoms. Then, we can replace the correlation function $G_{\mu\nu}(\tau)$ in Eq. (9) with the δ function with respect to the time scale of interest, which means that we are interested only in calculating the integral value $N_{\mu\nu}=\int_{-\infty}^{\infty}G_{\mu\nu}(\tau)d\tau$. The spectral width of the atomic emission fluctuations under the integral in Eq. (9) is narrow with respect to that of the fluctuations of the vacuum electromagnetic field, so that one can simply use the correlation function $\mathcal{K}_s(\tau)=\langle\sigma_{s\mu}^{-}\sigma_{s\mu}^{+}\rangle\exp(-\omega_s t)$ in Eq. (9) and neglect the Doppler shift term for the same reason. As a result, the power spectral density $N_{\mu\nu}$ of the correlation function $G_{\mu\nu}(\tau)$ takes the form

$$N_{\mu\nu}=\sum_s\frac{\hbar\omega_s^5 d_s^2}{2\pi c^5}\langle\Delta\sigma_{s\mu}^{-}\Delta\sigma_{s\nu}^{+}\rangle\times\int\mathbf{e}_{\perp s}^{\mu}\cdot\mathbf{e}_{\perp s}^{\nu}\exp(-i\omega_s\mathbf{n}\mathbf{R}_{\nu\mu})\mathbf{n}\mathbf{n}^{\mathrm{T}}d\mathbf{n}\qquad\text{(B1)}$$

with the correlation function $\langle\Delta\sigma_{s\mu}^{-}\Delta\sigma_{s\nu}^{+}\rangle$ of the sth atomic transition operator being nonzero due to the correlations caused by the virtual photon exchange between the atoms (DDI). The DDI term also enters into the multiatomic relaxation operator derived in Appendix C.

For the case of the atomic dipole moments parallel to each other and orthogonal to the vector of displacement between the atoms, i.e.,

$$\mathbf{e}_{\perp s}^{\mu}\parallel\mathbf{e}_{\perp s}^{\nu}\perp\mathbf{R}_{\mu\nu},\qquad\text{(B2)}$$

the integral in Eq. (B1), which we will denote as I, can be expressed analytically in a simple way:

$$I=\int\mathbf{e}_{\perp s}^{\mu}\cdot\mathbf{e}_{\perp s}^{\nu}\exp(-i\omega_s\mathbf{n}\mathbf{R}_{\nu\mu})\mathbf{n}\mathbf{n}^{\mathrm{T}}d\mathbf{n}=\pi\begin{pmatrix}\tilde{I}_1&0&0\\0&\tilde{I}_2&0\\0&0&\tilde{I}_3\end{pmatrix}\qquad\text{(B3)}$$

with

$$\tilde{I}_1=\frac{4\left(9-\varphi_{\mu\nu}^2\right)\cos\varphi_{\mu\nu}}{\varphi_{\mu\nu}^4}-\frac{4\left(9-4\varphi_{\mu\nu}^2\right)\sin\varphi_{\mu\nu}}{\varphi_{\mu\nu}^5},$$
$$\tilde{I}_2=\frac{4\left(3-\varphi_{\mu\nu}^2\right)\cos\varphi_{\mu\nu}}{\varphi_{\mu\nu}^4}-\frac{4\left(3-2\varphi_{\mu\nu}^2\right)\sin\varphi_{\mu\nu}}{\varphi_{\mu\nu}^5},\qquad\text{(B4)}$$
$$\tilde{I}_3=\frac{-4\left(12-3\varphi_{\mu\nu}^2\right)\cos\varphi_{\mu\nu}}{\varphi_{\mu\nu}^4}+\frac{4\left(12-7\varphi_{\mu\nu}^2+\varphi_{\mu\nu}^4\right)\sin\varphi_{\mu\nu}}{\varphi_{\mu\nu}^5},$$

where $\varphi_{\mu\nu}=\omega_s R_{\mu\nu}/c$, and the z and x axes are set along the $R_{\mu\nu}$ and the atomic dipole moment, respectively.

After calculation of the integral in Eq. (B1), the power spectral density $N_{\mu\nu}$ simplifies to

$$N_{\mu\nu}=\frac{3\pi\hbar^2}{8c^2}\sum_s\gamma_s\omega_s^2\langle\Delta\sigma_{s\mu}^{-}\Delta\sigma_{s\nu}^{+}\rangle I\to\frac{\hbar^2}{5c^2}\sum_s\gamma_s\omega_s^2\langle\Delta\sigma_{s\mu}^{-}\Delta\sigma_{s\nu}^{+}\rangle(P_s^{\parallel}+2P_s^{\perp}),\qquad\text{(B5)}$$

where, in contrast to Eq. (A3) for the power spectral density of the correlation function for a single atom, the single-atom dispersion is replaced with the interatomic correlation: $n_s-\langle\hat{\sigma}_s^{-}\rangle\langle\hat{\sigma}_s^{+}\rangle\to\langle\Delta\sigma_{s\mu}^{-}\Delta\sigma_{s\nu}^{+}\rangle$. It also follows from Eq. (B5) that the force fluctuations are correlated if there are correlations between incoherent oscillations of the atomic dipole transitions.

APPENDIX C: CALCULATION OF THE RADIATION RELAXATION LIOUVILLIAN

The relaxation superoperator $\mathcal{L}_{\mathrm{rel}}$, or the so-called radiation relaxation Liouvillian, of the diffusion stochastic process in the form of the average second commutator is

$$\mathcal{L}_{\mathrm{rel}}=-\lim_{\Delta\to0}\frac{1}{\hbar^2\Delta}\int_0^{\Delta}d\tau_2\int_0^{\tau_2}\left\langle\left[\sum_k\left(\hat{\sigma}_k^{+}\hat{\xi}_{k\tau_1}^{-}+\hat{\sigma}_k^{-}\hat{\xi}_{k\tau_1}^{+}\right),\left[\sum_m\left(\hat{\sigma}_m^{+}\hat{\xi}_{m\tau_2}^{-}+\hat{\sigma}_m^{-}\hat{\xi}_{m\tau_2}^{+}\right),\odot\right]\right]\right\rangle d\tau_1,\qquad\text{(C1)}$$

where $\hat{\sigma}^{\pm}$ are the atomic transition operators, $\hat{\xi}^{\pm}$ are the reservoir noises (due to the interaction of atoms with the vacuum field) acting on the corresponding atomic transitions, and the substitution symbol $\odot$ should be replaced by the transforming operator variable. The above relation can be recast in the form

$$\mathcal{L}_{\mathrm{rel}}=\sum\mathcal{L}_k+\sum_{k\neq m}\mathcal{L}_{km},\qquad\text{(C2)}$$

where the first sum describes the radiative decay of individual atoms in the trap, and the second sum represents the DDI between pairs of atoms due to the exchange of virtual photons between them via the vacuum electromagnetic field [44,55]. Here

$$\mathcal{L}_{km}=-\frac{\gamma_{kl}}{2}(\hat{\sigma}_k^{-}\hat{\sigma}_m^{+}\odot+\odot\,\hat{\sigma}_k^{-}\hat{\sigma}_m^{+}-\hat{\sigma}_k^{-}\odot\hat{\sigma}_m^{+}-\hat{\sigma}_m^{-}\odot\hat{\sigma}_k^{+}),\qquad\text{(C3)}$$

where we omitted the analog of the Lamb shift, and

$$\gamma_{kl}=\lim\frac{2}{\hbar^2\Delta}\int_0^{\Delta}\int_0^{\tau_2}\mathrm{Re}\,e\langle\hat{\xi}_{k\tau_1}^{+}\hat{\xi}_{m\tau_2}^{-}\rangle d\tau_1 d\tau_2=\int_{-\infty}^{\infty}\int\frac{\omega}{4\hbar\pi^2}\mathbf{d}_{\perp}^{k}\cdot\mathbf{d}_{\perp}^{m}\exp[i(\omega-\omega_{\mathrm{a}})\tau-i\mathbf{k}\hat{\mathbf{R}}_{km}]d\mathbf{k}\,d\tau=\frac{\omega_{\mathrm{a}}^3}{2\pi\hbar c^3}\int\mathbf{d}_{\perp}^{k}\cdot\mathbf{d}_{\perp}^{m}\exp(-i\omega_{\mathrm{a}}\mathbf{n}\hat{\mathbf{R}}_{km}/c)d\mathbf{n}.\qquad\text{(C4)}$$

For the geometry specified in Eq. (B2), Eq. (C4) simplifies to

$$\gamma_{kl}=\gamma_0\zeta,\quad\zeta=\frac{3}{2}\frac{\varphi\cos\varphi-\sin\varphi+\varphi^2\sin\varphi}{\varphi^3},\qquad\text{(C5)}$$

where $\varphi=\omega_{\mathrm{a}}R_{kl}/c$ and γ_0 is the atomic decay rate [56].

In the absence of the near-resonant probe laser excitation, the relaxation superoperator (C3) can be simplified by introducing symmetric and antisymmetric types $\hat{e}_k \otimes \hat{e}_l \pm \hat{e}_l \otimes \hat{e}_k$ of the dynamic variables in the eigenbasis $\hat{e}$ of the relaxation superoperator. In the case of two-level atoms in the single-atom basis of dimension $n = 4$, for example, we get 16 elements with the two-atomic basis, including four diagonal basis elements $\hat{e}_k \otimes \hat{e}_k$, six symmetric and six antisymmetric. Keeping in mind that any physically feasible evolution operator always has zero matrix elements between the symmetric and antisymmetric subspaces, one can reduce it to 10-dimensional space. In the general case of $\zeta < 1$, the corresponding 10 eigenvalues are listed below:

$$\lambda = \gamma_0\Big(0,-1+\zeta,-\frac{1+\zeta}{2},-\frac{1+\zeta}{2},-1,-1,-1-\zeta,-\frac{3+\zeta}{2},-\frac{3+\zeta}{2},-2\Big). \tag{C6}$$

Hence, for the closely spaced atoms ($\zeta = 1$), there are only two independent stationary states, corresponding to $\lambda_0 = 0$ and $\lambda_1 = -1 + \zeta = 0$, respectively. The eigendensity matrix basis elements, corresponding to these two zero eigenvalues, are

$$\hat{\rho}_0 = \begin{pmatrix} 1 & 0 & 0 & 0 \\ 0 & 0 & 0 & 0 \\ 0 & 0 & 0 & 0 \\ 0 & 0 & 0 & 0 \end{pmatrix} \quad \text{and} \quad \hat{\rho}_1 = \begin{pmatrix} -1 & 0 & 0 & 0 \\ 0 & \frac{1}{2} & -\frac{1}{2} & 0 \\ 0 & -\frac{1}{2} & \frac{1}{2} & 0 \\ 0 & 0 & 0 & 0 \end{pmatrix}, \tag{C7}$$

respectively. Here we used the wave-function basis $|00\rangle$, $|01\rangle$, $|10\rangle$, and $|11\rangle$, where "0" and "1" mark the atomic ground and excited states, respectively. The first matrix in Eq. (C7) corresponds to the two-atomic vacuum state, while the second one corresponds to the sum of the density matrix of the ground state $|00\rangle$ (with negative sign) and the coherent antisymmetric excitation of both interacting atoms. The corresponding eigenbasis $\hat{e}_k$ of the physical variables has an identity matrix equal to the null eigenvector and the matrix

$$\hat{e}_1 = \begin{pmatrix} 0 & 0 & 0 & 0 \\ 0 & \frac{1}{2} & -\frac{1}{2} & 0 \\ 0 & -\frac{1}{2} & \frac{1}{2} & 0 \\ 0 & 0 & 0 & \frac{1-g}{1+g} \end{pmatrix}, \tag{C8}$$

corresponding to the $1-\zeta$ eigenvalue. The null eigenvector represents an antisymmetric coherent excitation with the population of the excited state given by $(1 - xi)/(1 + \zeta)$.

APPENDIX D: CALCULATION OF THE LASER LIOUVILLIAN

The dynamics of an atom driven by a probe near-resonant laser field is described by free precession with the laser frequency ω_L and the corresponding contribution $\mathcal{L}_L$ to the total Liouvillian, which, in the rotating wave approximation (RWA), has the form

$$\mathcal{L}_L = i\sum_\mu \frac{g_{L\mu}}{2}[\hat{\sigma}_{1\mu},\odot] - i\sum_\mu \frac{\delta_L}{2}[\hat{\sigma}_{3\mu},\odot], \tag{D1}$$

where $\hat{\sigma}_{1\mu},\hat{\sigma}_{3\mu}$ are the Pauli matrices for the μth atom, $g_{L\mu}$ is the corresponding Rabi frequency, and δ_L is the frequency detuning of the probe laser field.

For the geometry specified in Eq. (B2), we have $g_{L\mu} = g_L$. Then, using a 10-dimensional representation of the total superoperator $\mathcal{L} = \mathcal{L}_{rel} + \mathcal{L}_L$, one can calculate its eigenvalues and the stationary null-space vector. The corresponding stationary density matrix has the form

$$\hat{\rho} = \begin{pmatrix} \frac{A_1}{A_0} & \frac{\tilde{g}_L(i+2\tilde{\delta}_L)A_2}{A_0} & \frac{\tilde{g}_L(2\tilde{\delta}_L+i)A_2}{A_0} & \frac{\tilde{g}_R^2(2\tilde{\delta}_L+i)(2\tilde{\delta}_L+i+i\zeta)}{A_0} \\ \frac{\tilde{g}_L(2\tilde{\delta}_L-i)A_2^*}{A_0} & \frac{\tilde{g}_L^2(1+4\tilde{\delta}_L^2+\tilde{g}_L^2)}{A_0} & \frac{\tilde{g}_L^2(1+4\tilde{\delta}_L^2)}{A_0} & \frac{\tilde{g}_L^3(2\tilde{\delta}_L+i)}{A_0} \\ \frac{\tilde{g}_L(2\tilde{\delta}_L-i)A_2^*}{A_0} & \frac{\tilde{g}_L^2(1+4\tilde{\delta}_L^2)}{A_0} & \frac{\tilde{g}_L^2(1+4\tilde{\delta}_L^2+\tilde{g}_L^2)}{A_0} & \frac{\tilde{g}_L^3(2\tilde{\delta}_L+i)}{A_0} \\ \frac{\tilde{g}_L^2(2\tilde{\delta}_L-i)(2\tilde{\delta}_L-i-i\zeta)}{A_0} & \frac{\tilde{g}_L^3(2\tilde{\delta}_L-i)}{A_0} & \frac{\tilde{g}_L^3(2\tilde{\delta}_L-i)}{A_0} & \frac{\tilde{g}_L^4}{A_0} \end{pmatrix}, \tag{D2}$$

where $\tilde{g}_L = g_L/\gamma_0, \tilde{\delta}_L = \delta/\gamma_0$, and

$$A_0 = (1+\zeta)^2 + 4\big(\tilde{g}_L^2 + \tilde{\delta}_L^2\big) + 4(1+\zeta)^2\tilde{\delta}_L^2 + 4\big(\tilde{g}_L^2 + 2\tilde{\delta}_L^2\big)^2,$$
$$A_1 = (1+\zeta)^2 + 2\big(\tilde{g}_L^2 + 2\tilde{\delta}_L^2\big) + 4(1+\zeta)^2\tilde{\delta}_L^2 + \big(\tilde{g}_L^2 + 4\tilde{\delta}_L^2\big)^2,$$
$$A_2 = 1 + 4\tilde{\delta}_L^2 + \zeta + 2i\tilde{\delta}_L\zeta + \tilde{g}_L^2.$$

By using the two-atom density matrix (D2), one can calculate any characteristic of the internal atomic dynamics, including the correlation matrix $\mathcal{K}_s(\tau) = \langle\sigma_{s\mu}^-\sigma_{s\mu}^+\rangle \exp(-\omega_s t)$, which is used to determine the force correlation matrix (9).

[1] V. S. Letokhov, JETP Lett. **7**, 272 (1968).

[2] C. S. Adams and E. Riis, Prog. Quantum Electron. **21**, 1 (1997).

[3] H. K. Metcalf and P. van der Straten, *Laser Cooling and Trapping* (Springer-Verlag, New York, 1999), p. 150.

[4] V. I. Balykin, V. G. Minogin, and V. S. Letokhov, Rep. Prog. Phys. **63**, 1429 (2000).

[5] R. Grimm, M. Weidemuller, and Y. B. Ovchinnikov, Adv. At. Mol. Opt. Phys. **42**, 95 (2000).

[6] I. Bloch, Nature (London) **453**, 1016 (2008).
[7] J. Y. Kim, J. S. Lee, J. H. Han, and D. Cho, J. Korean Phys. Soc. **42**, 483 (2003).
[8] M. Takamoto, F. L. Hong, R. Higashi, and K. Katori, Nature (London) **435**, 321 (2005).
[9] T. G. M. Freegarde, J. Waltz, and T. W. Hänsch, Opt. Commun. **117**, 262 (1995).
[10] A. Goepfert, I. Bloch, D. Haubrich, F. Lison, R. Schütze, R. Wynands, and D. Meschede, Phys. Rev. A **56**, R3354 (1997).
[11] R. B. M. Clarke, T. Graf, and E. Riis, Appl. Phys. B **70**, 695 (2000).
[12] M. Shiddiq, E. M. Ahmed, M. D. Havey, and C. I. Sukenik, Phys. Rev. A **77**, 045401 (2008).
[13] J. M. Choi, G.-N. Kim, D. Cho, and C. I. Sukenik, J. Korean Phys. Soc. **51**, 294 (2007).
[14] J. M. Choi, G.-N. Kim, and D. Cho, Phys. Rev. A **77**, 010501(R) (2008).
[15] J. Weiner, V. S. Bagnato, S. Zilio, and P. S. Julienne, Rev. Mod. Phys. **71**, 1 (1999).
[16] J. Piilo and K.-A. Suominen, J. Opt. B **7**, R37 (2005).
[17] G. W. King and J. H. Van Vleck, Phys. Rev. **55**, 1165 (1939).
[18] H. B. G. Casimir and D. Polder, Phys. Rev. **73**, 360 (1948).
[19] M. J. Stephen, J. Chem. Phys. **40**, 699 (1964).
[20] P. W. Milonni and P. L. Knight, Phys. Rev. A **10**, 1096 (1974).
[21] A. M. Smith and K. Burnett, J. Opt. Soc. Am. B **8**, 1592 (1991).
[22] G. Lenz and P. Meystre, Phys. Rev. A **48**, 3365 (1993).
[23] E. V. Goldstein, P. Pax, and P. Meystre, Phys. Rev. A **53**, 2604 (1996).
[24] C. Menotti and H. Ritsch, Phys. Rev. A **60**, R2653 (1999).
[25] A. M. Guzman and P. Meystre, Phys. Rev. A **57**, 1139 (1998).
[26] P. R. Berman, Phys. Rev. A **55**, 4466 (1997).
[27] D. N. Yanyshev, B. A. Grishanin, V. N. Zadkov, and D. Meschede, Laser Phys. **15**, 1189 (2005).
[28] T. F. Gallagher and P. Pillet, *Advances in Atomic, Molecular, and Optical Physics*, Vol. 56 (Elsevier, Amsterdam, 2008), Chap. 4.
[29] D. Comparat and P. Pillet, J. Opt. Soc. Am. B **27**, 208 (2010).
[30] A. Gallagher and D. E. Pritchard, Phys. Rev. Lett. **63**, 957 (1989).
[31] M. Machholm, P. S. Julienne, and K.-A. Suominen, Phys. Rev. A **64**, 033425 (2001).
[32] J. L. Carini, J. A. Pechkis, C. E. Rogers III, P. L. Gould, S. Kallush, and R. Kosloff, Phys. Rev. A **85**, 013424 (2012).
[33] L. Förster, W. Alt, I. Dotsenko, M. Khudaverdyan, D. Meschede, Y. Miroshnychenko, S. Reick, and A. Rauschenbeutel, New J. Phys. **8**, 259 (2006).
[34] A. Fuhrmanek, R. Bourgain, Y. R. P. Sortais, and A. Browaeys, Phys. Rev. A **85**, 062708 (2012).
[35] Y. R. P. Sortais, A. Fuhrmanek, R. Bourgain, and A. Browaeys, Phys. Rev. A **85**, 035403 (2012).
[36] V. I. Balykin, JETP Lett. **81**, 268 (2005).
[37] B. V. Chirikov, Phys. Rep. **52**, 263 (1965).
[38] M. G. Raizen, Adv. Mol. Opt. Phys. **41**, 43 (1999).
[39] T. E. Lee, H. Häffner, and M. C. Cross, Phys. Rev. Lett. **108**, 023602 (2012).
[40] V. I. Romanenko and L. P. Yatsenko, J. Phys. B **44**, 115305 (2011).
[41] I. S. Tarakanov, V. I. Balykin, Yu. V. Vladimirova, D. N. Yanyshev, and V. N. Zadkov, in *ICONO 2010: International Conference on Coherent and Nonlinear Optics*, in *Proceedings of SPIE 7993*, edited by C. Fabre, V. N. Zadkov, and K. N. Drabovich (SPIE, Bellingham, 2011), p. 799316.
[42] T. Brabec and F. Krausz, Rev. Mod. Phys. **72**, 545 (2000).
[43] B. Uberholz, S. Kuhr, D. Frese, D. Meschede, and V. Gomer, J. Phys. B **33**, L135 (2000).
[44] C. W. Gardiner and P. Zoller, *Quantum Noise. A Handbook of Markovian and Non-Markovian Quantum Stochastic Methods with Applications to Quantum Optics* (Springer-Verlag, Berlin, 2000), Chap. 9.
[45] H.-P. Breuer and F. Petruccione, *The Theory of Open Quantum Systems* (Oxford University Press, New York, 2003).
[46] A. M. Steane, M. Chowdhury, and C. J. Foot, J. Opt. Soc. Am. B **9**, 2142 (1992).
[47] I. V. Bargatin, B. A. Grishanin, and V. N. Zadkov, Phys. Usp. **44**, 597 (2001).
[48] I. V. Bargatin, B. A. Grishanin, and V. N. Zadkov, Fortsch. Phys. **48**, 637 (2000).
[49] I. V. Bargatin, B. A. Grishanin, and V. N. Zadkov, Phys. Rev. A **61**, 052305 (2000).
[50] Th. Sauter, W. Neuhauser, R. Blatt, and P. E. Toschek, Phys. Rev. Lett. **57**, 1696 (1986).
[51] S. U. Addicks, A. Beige, M. Dakhna, and G. C. Hegerfeldt, Eur. Phys. J. D **15**, 393 (2001).
[52] V. Hannestein and G. C. Hegerfeldt, Eur. Phys. J. D **38**, 415 (2006).
[53] R. G. DeVoe and R. G. Brewer, Phys. Rev. Lett. **76**, 2049 (1996).
[54] G. Kurizki, Phys. Rev. A **43**, 2599 (1991).
[55] B. A. Grishanin, in *B. A. Grishanin: Selected Works and Rememberings of His Relatives, Friends, and Colleagues*, edited by V. N. Zadkov and Yu. M. Romanovski (Lomonosov Moscow State University Press, Moscow, 2011), Pt. IV.
[56] Different orientation geometries of the dipole moments of two interacting atoms and averaging over them are considered in Ref. [57].
[57] S. I. Schmid and J. Evers, Phys. Rev. A **77**, 013822 (2008).